Supplementary materials

Andrea Piccoli[1,2 *], Valentina Agresti[2], Giovanni Lonati[1] and Guido Pirovano[2].
[1] Department of Civil and Environmental Engineering, Politecnico di Milano, Milan, Piazza L. Da Vinci 32, 20133, Italy.
[2] Sustainable Development and Energy Sources, RSE Spa, Milan, Via R. Rubattino 54, 20134, Italy.

S1 – Additional information on the setting of the puff's initial conditions

As explained in the main text, the goal of LPiG is to simulate the concentration of a linear source by adapting the original PiG module of CAMx. The first step to simulate a linear source is to define the initial condition of the puff at the end of the emission period. For this scope, we can imagine the road as an infinite number of point sources that covers the road surface. In order to work in the PiG framework, we need to represent a linear source puff as a puff originated by a single associated point source (synpuff in the main text). The center point of the linear source puff and the one of the associated point sources has the same coordinates and is defined in equation 1.

The vector coordinates $\underline{x}_{T_s,0}$ and $\underline{x}_{L_s,0}$ are calculated based on the vector coordinate of the leading and trailing point of the puff emitted by the associated point source $\underline{x}_{L_{aps}}$, $\underline{x}_{T_{aps}}$) and on two correction vectors in order to account for the actual length (L_s) and width (W_s) of the linear source. To this aim, we need to introduce three unit vectors in the horizontal plane: the wind unit vector $\underline{u}_{hn}$ and two unit vectors $\underline{s}$ and $\underline{n}$, respectively aligned with the major and minor road axis. These three unit vectors are computed as:

$$\underline{s} = \frac{\underline{x}_{Rd1} - \underline{x}_{Rd2}}{\left|\underline{x}_{Rd1} - \underline{x}_{Rd2}\right|}, \quad \underline{n} = \underline{s} \times \underline{k}, \quad \underline{u}_{hn} = \frac{\underline{x}_{L_{aps}} - \underline{x}_{T_{aps}}}{\left|\underline{x}_{L_{aps}} - \underline{x}_{T_{aps}}\right|} \tag{S1}$$

where $\underline{k}$ is the unit vector aligned with the vertical, $\underline{x}_{Rd1}$ and $\underline{x}_{Rd2}$ are the vector coordinates of the two road vertices, $\underline{x}_{L_{aps}}$ and $\underline{x}_{T_{aps}}$ are the vector coordinates of the puff leading and trailing point of the associated point source at the end of the emission period. The angle between $\underline{u}_{hn}$ and $\underline{s}$ is α, while the angle between $\underline{u}_{hn}$ and $\underline{n}$ is ϑ. The correction vectors $\underline{L_{corr}}$ (parallel to the major axis of the road) and $\underline{W_{corr}}$ (normal to the road segment) defined as follows:

$$\underline{L_{corr}} = \frac{L_s}{2} \cos\alpha \ \underline{s} \tag{S2}$$

$$\underline{W_{corr}} = sign(\cos\vartheta)\frac{W_s}{2} \sin\alpha \ \underline{n} \tag{S3}$$

If the length and width of the linear source are null ($L_s = W_s = 0$), then the corrective vectors $\underline{L_{corr}}$ and $\underline{W_{corr}}$ are null as well, and the scheme LPiG degenerates in the scheme PiG.

The vector coordinates of the trailing and leading point of the synpuff are then computed as:

$$\begin{aligned} \underline{x}_{T_s,0} &= \underline{x}_{T_{aps},0} - \underline{L_{corr}} - \underline{W_{corr}} \\ \underline{x}_{L_s,0} &= \underline{x}_{L_{aps},0} + \underline{L_{corr}} + \underline{W_{corr}} \end{aligned} \tag{S4}$$

When the wind direction is perpendicular to the road segment (Figure S 1), we have α = 90° and ϑ = 0°, so that $\underline{L_{corr}} = 0$ and $\underline{W_{corr}} = {}^{W_s}/_2 \ \underline{n}$; thus, the only difference between the leading and trailing point of the linear source and those of the associated point source is only due to $\underline{W_{corr}}$. $\underline{x}_{L_{aps}}$ and $\underline{x}_{T_{aps}}$ are then corrected by adding/subtracting half the width of the road in the $\underline{n}$ direction.

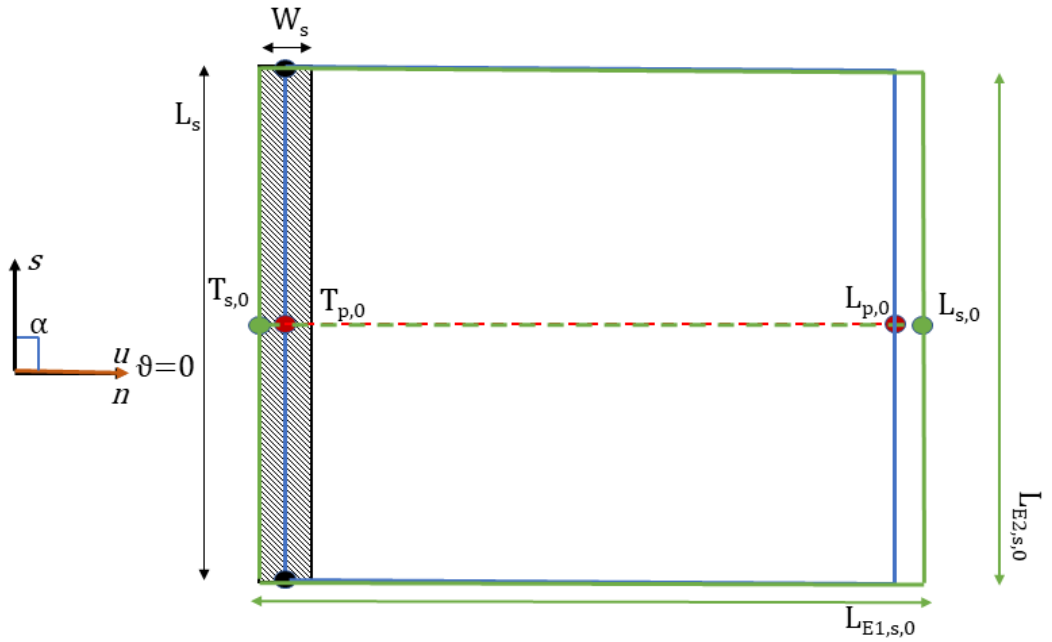

Figure S 1 - Definition of the puff geometry in case of wind direction normal to the street segment. The road segment is reported as the stripped black area, the leading and trailing points of the associated point source are in red, while the leading and trailing points of street source are in green. The quadrilaterals in blue and green represent the initial smoke surface due to the mean motion of the puff for the associated point source and the street source, respectively.

Conversely, when the wind is parallel to the road segment (α = 0° and ϑ = 90°), we have $\underline{L_{corr}} = {}^{L_s}/_2 \ \underline{s}$ and $\underline{W_{corr}}$ = 0 (Figure S 2); thus, $\underline{x}_{L_{aps},0}$ and $\underline{x}_{T_{aps},0}$ are corrected by adding/subtracting $L_s/2$ in the $\underline{s}$ direction.

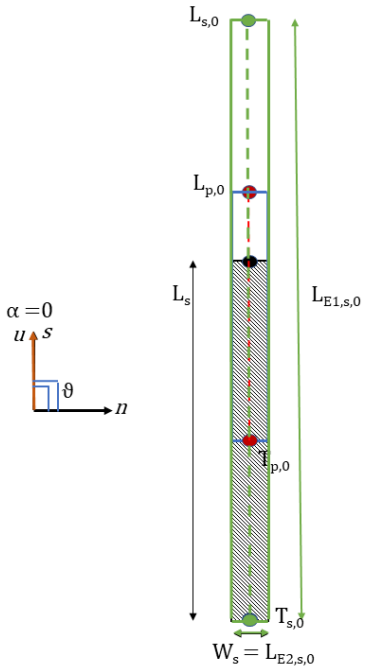

Figure S 2 - Definition of the puff geometry in case of wind direction parallel to the street segment. The road segment is reported as the stripped black area, the leading and trailing points of the associated point source are in red, while the leading and trailing points of street source are in green. The quadrilaterals in blue and green represent the initial smoke surface due to the mean motion of the puff for the associated point source and the street source, respectively.

In a general wind configuration (Figure S 3) both the correction vectors for road width ($\underline{W_{corr}}$) and length ($\underline{L_{corr}}$) affect the vector coordinates $\underline{x}_{L_s,0}$ and $\underline{x}_{T_s,0}$.

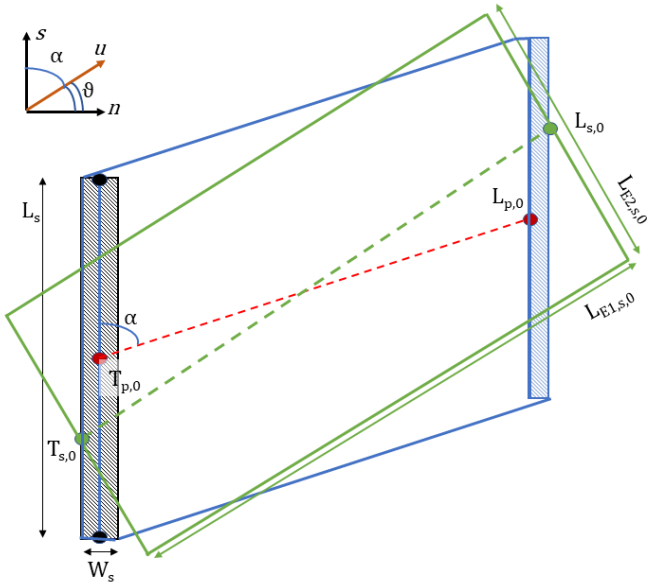

Figure S 3 - Definition of the puff geometry in case of generic wind direction. The road segment is reported as the stripped black area, the leading and trailing points of the associated point source are in red, while the leading and trailing points of street source are in green. The quadrilaterals in blue and green represent the initial smoke surface due to the mean motion of the puff for the associated point source and the street source, respectively.

Once the trailing and leading point are corrected, we need to find the two dimensions of the puff, the major effective length Le1s and the minor effective length. The major effective length is defined as the length of the puff along the x axis of the puff's local coordinate system (green dashed lines of Figure S 3). This length it's the distance between the leading and trailing point:

$$L_{E1,s} = \left|\underline{x}_{L_s,0} - \underline{x}_{T_s,0}\right|$$

To find the minor effective length, or the length along its y axis, we assume that the puff has a rectangular shape and an area that is equal to the blue area in Figure S 1, Figure S 2 and Figure S 3 plus the area of the street source. The minor effective length is therefore computed as:

$$L_{E2,s} = \frac{L_s \cdot \left|\underline{x}_{T_{aps}} - \underline{x}_{L_{aps}}\right| \cdot |\sin\alpha| + W_s \left|\underline{x}_{T_{aps}} - \underline{x}_{L_{aps}}\right| \cdot |\cos\alpha| + L_s \cdot W_s}{L_{E1,s}}$$

S2 – Test case results for the modified emission timestep

In Figure S 4, the comparison between two LPiG simulation for a test case for 82 street in the center of Milan for January 2010 Is presented. In the left panel there is the mean concentration for the LPiG simulation with the original emission timestep, while in the right panel there is the relative differences between the original emission timestep and the modified one. In Table S 1 the mean computation time for the test case shown in Figure S 4 and for a test case with more road links that are explicitly simulated is reported.

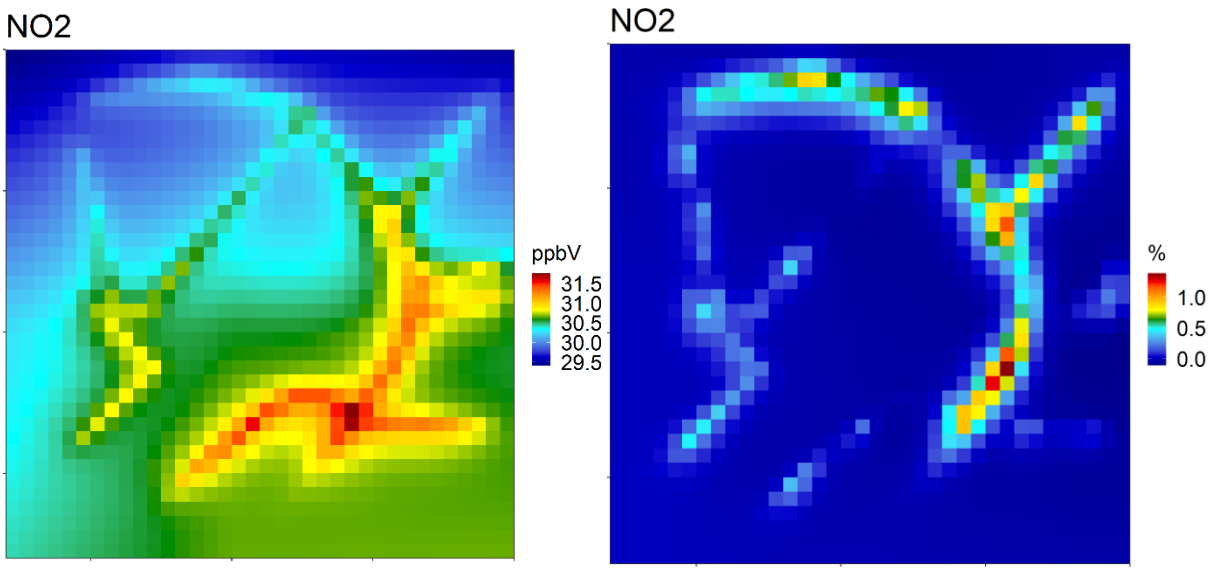

Figure S 4 – Left panel: Mean January 2010 concentration for a test case in the city center of Milan, right panel: Relative difference between the two methods of emitting the puffs

Table S 1 – Comparison of the computational time needed to simulate one day of LPiG with different number of road links.

N° of Road Links	Original LPiG	Modified LPiG
82	4h 24m	1h 1m
515	2d 19h 20m	6h 10m

As we can see the maximum differences is low, circa 1.5% while the computational benefits are high. The time needed for a single day decrease of 77% with 82 road links and of 90% with 515

S3 -Tables and Figures in support to the model validation of Chapter 3

Table S 2 – CAMx validation for daily NO2 values for the month of January 2017

AQ site	Coverage	Obs	Mod	Mean Bias	RMSE	NMB	COR	IOA
	%	ppbV	ppbV	ppbV	ppbV	%	-	-
S1	100	39.89	33.20	-6.69	10.53	-16.78	0.567	0.68
S2	74	37.77	32.07	-5.69	12.23	-15.08	0.302	0.53
S3	100	40.92	33.65	-7.27	10.18	-17.78	0.667	0.69

Figure S 5 - Daily NOX modeled concentration time series for the AQ stations of Viale Marche (IT0477A), Viale Liguria (IT0761A) and Via Senato (IT1016A) for January 2017. the red line represents the CAMX LPiG simulation and the green line represent the CAMx simulation.

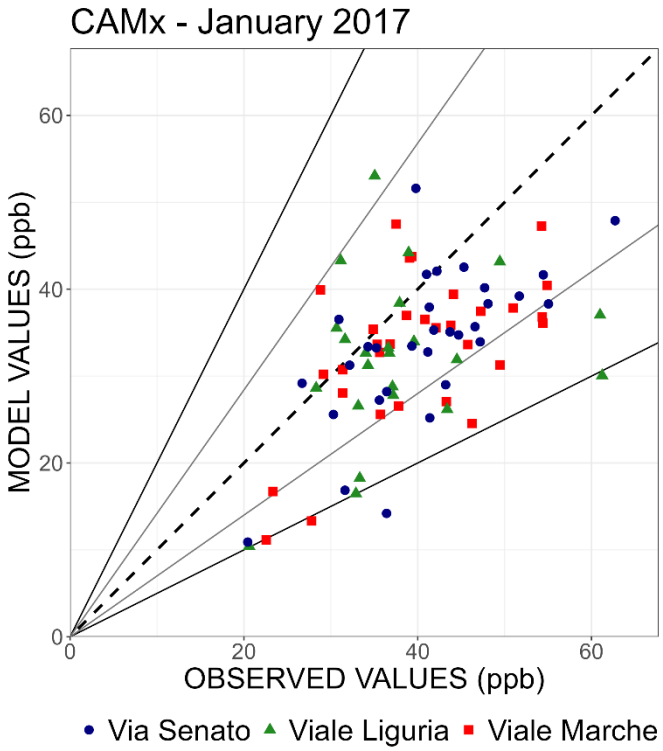

Figure S 6 - Scatter plot of Observed vs Modelled NO2 daily mean concentrations at the AQ site of Viale Marche, Viale Liguria and Via Senato for the CAMx simulation. The dashed line has a slope of 1, while the black lines have a slope of 2 and 0.5.

Table S 3 – CAMx validation for hourly NO2 values for the month of January 2017

AQ site	Coverage	Obs	Mod	Mean Bias	RMSE	NMB	COR	IOA
	%	ppbV	ppbV	ppbV	ppbV	%	-	-
S1	100	39.9	33.2	-6.7	16.2	-16.8	0.37	0.58
S2	75	38.3	32.2	-6.1	17.5	-16.0	0.41	0.62
S3	100	40.9	33.6	-7.3	15.5	-17.8	0.49	0.64

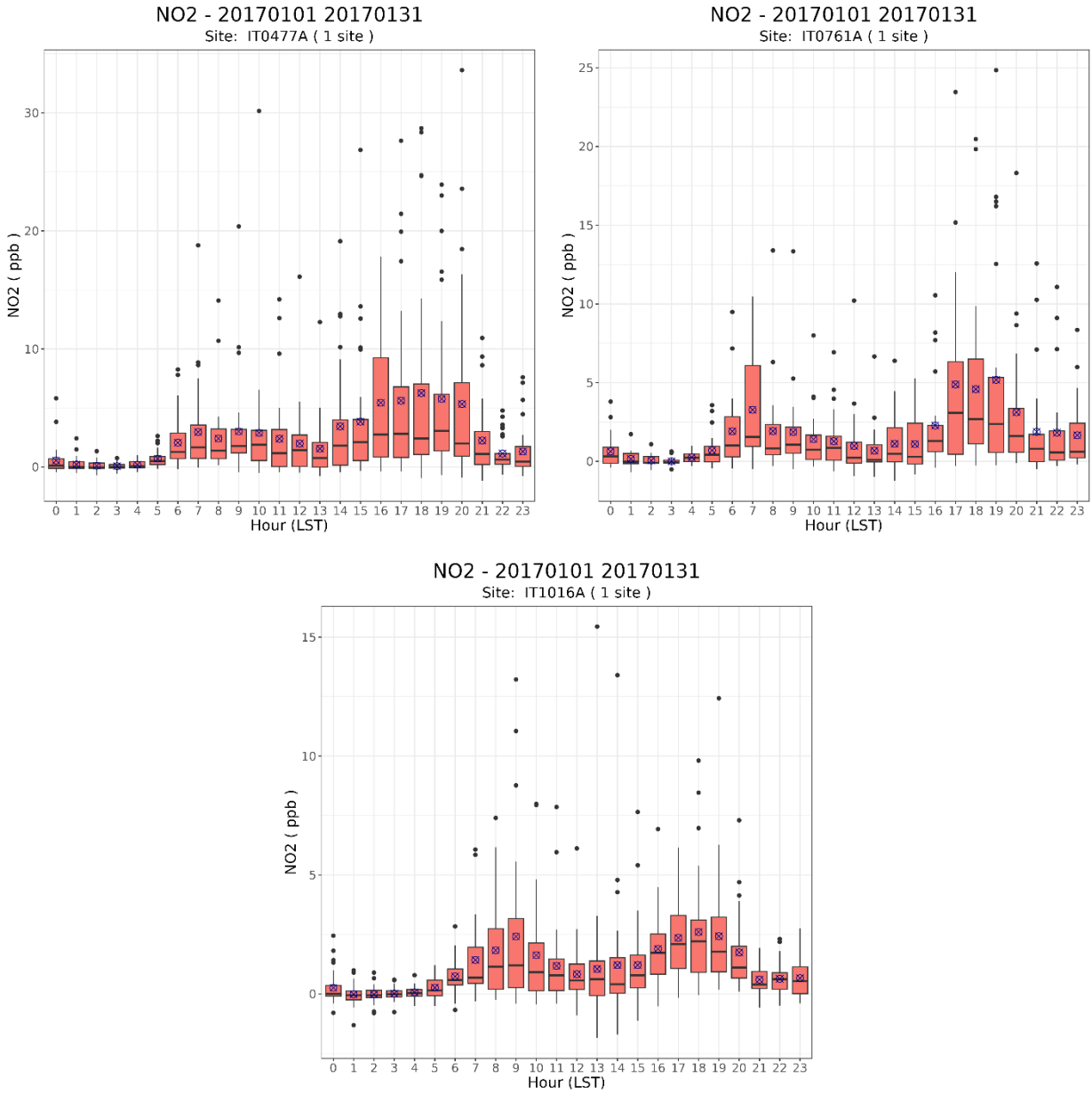

Figure S 7 – Hourly boxplot of NO2 difference in concentration between CAMx-LPiG and CAMx simulation for the AQ stations of Viale Marche (S1: IT0477A), Viale Liguria (S2: IT0761A) and Via Senato (S3: IT1016A) for January 2017. The mean difference at each hour is reported in blue

S4 - Figure in support to the discussion of Chapter 4

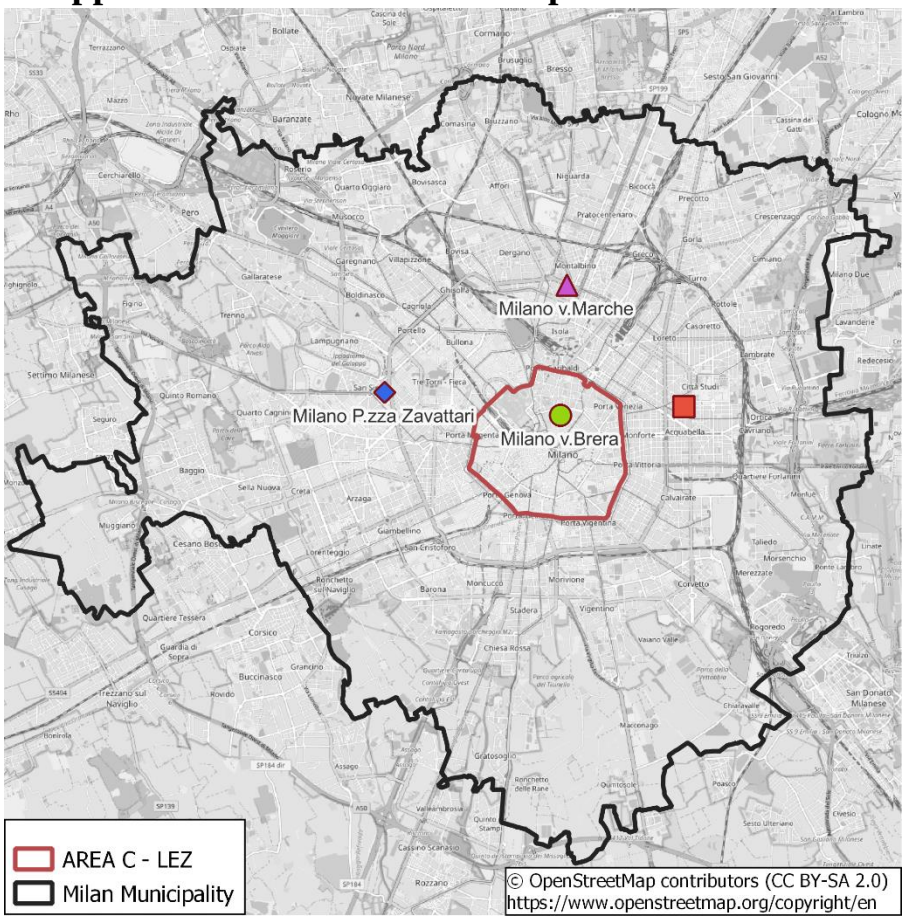

Figure S 8 – Location of the meteorological monitoring stations used in the validation of the WRF simulation

S5 - NOx validation for UT traffic station of Piazza Zavattari

For a more extensive validation of the model results, the results at an additional validation at the no longer active AQ monitoring site of Piazza Zavattari in the city of Milan is presented in this paragraph. The additional value of this validation is due to the availability of NOx measurements at the site. The site location is presented in Figure S 9. The station was of the Urban Traffic type and was situated in a secondary road close to the main road simulated with CAMx LPiG. For daily winter NOx concentrations (Figure S 10), the model performs better in the first period, followed by an underestimate in the central part of the month. When comparing CAMx and CAMX LPiG, we can see that the effect of the hybrid component is evident across the entire simulation period, and with the exception of the first quartile, it closes the gap with the observed monthly median, third and fourth quartiles. The hourly concentration validation is instead reported Figure S 11 for January 2017. The model is able to simulate the morning peak maximum value and lunch hour concentrations, but it overestimates the evening peak. In the Table S 4 the performance indices for NOx concentrations are reported. By comparing the performance of CAMx LPiG and CAMx, we can see that the hybrid model contributes to lowering the BIAS (NMB decrease from -9.42% to -2.62%) and improves the simulation of the observed standard deviation.

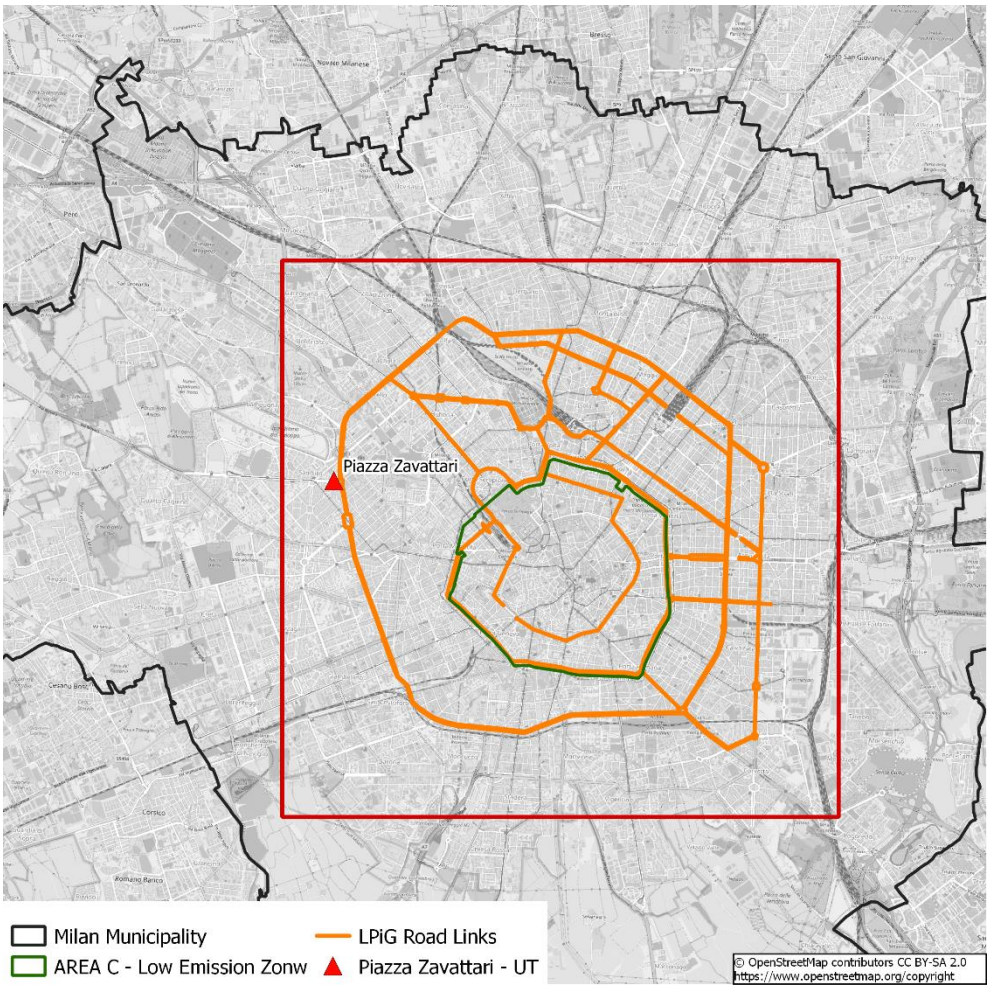

Figure S 9 – Location of AQ station of Piazza Zavattari (red triangle) and AREA C Low emission Zone (green)

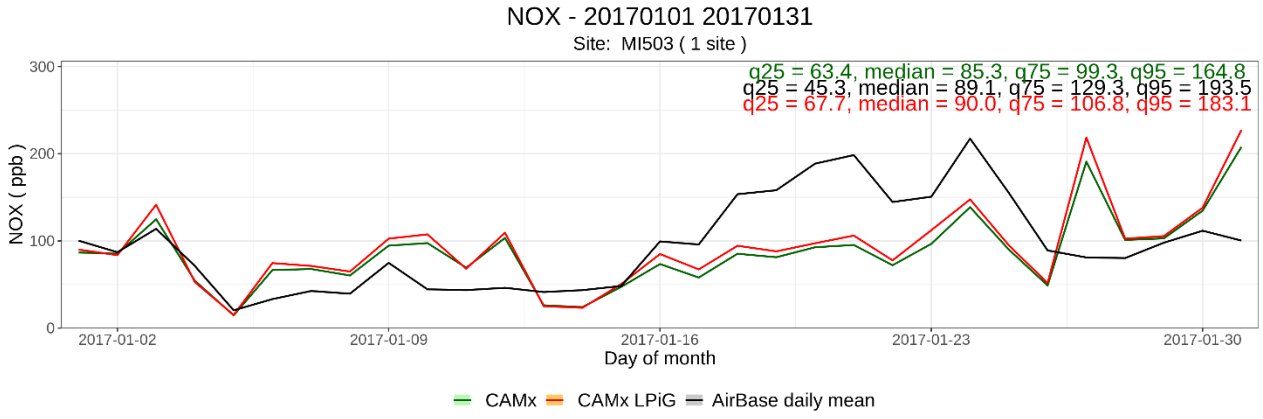

Figure S 10 - Daily NOX concentration time series for the AQ stations of Piazza Zavattari (MI503) for January 2017. The black line represents the observed value, the red line represents the CAMX LPiG simulation and the green line represent the CAMx simulation.

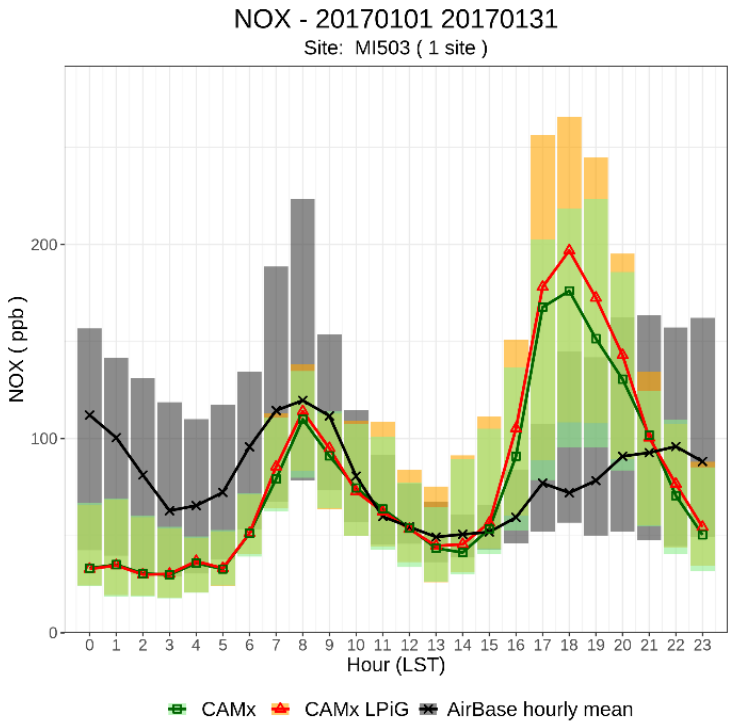

Figure S 11 - Hourly NOX concentration time series for the AQ stations of Piazza Zavattari (MI503) for January 2017. The black line represents the observed value, the red line represents the CAMX LPiG simulation and the green line represent the CAMx simulation. The boxes top and bottom values are the first and third quartiles.

Table S 4 – CAMx LPiG and CAMx validation for daily NOX values for the month of January 2017

AQ site	Coverage	Obs	Mod	σ Obs	σ Mod	Mean Bias	RMSE	NMB	COR	IOA
	%	ppbV	ppbV	ppbV	ppbV	ppbV	ppbV	%	-	-
LPiG	100	95.89	93.37	52.82	47.08	-2.52	54.72	-2.62	0.386	0.59
CAMx	100	95.89	86.85	52.81	42.01	-9.03	53.24	-9.42	0.385	0.59